# Oxygen Binding Constants and Stepwise Enthalpies for Human and Bovine Hemoglobin at pH 7.6†

Craig R. Johnson, David W. Ownby, Stanley J. Gill,‡ and Kevin S. Peters*

*Department of Chemistry and Biochemistry, University of Colorado at Boulder, Box 215, Boulder, Colorado 80309*

*Received April 14, 1992; Revised Manuscript Received July 24, 1992*

ABSTRACT: A high-precision thin-layer gas-solution microcalorimeter has been developed to study the binding reactions of gaseous ligands with ligand-binding macromolecules in a manner analogous to that of the Gill thin-layer optical apparatus [Doleman & Gill (1976) *Anal. Biochem. 87*, 127]. We have generated differential heat-binding curves of oxygen binding to human and bovine hemoglobin in phosphate buffer at pH 7.6, with the enzyme-reducing system of Hayashi et al. [(1973) *Biochim. Biophys. Acta 310*, 309]. Experiments were conducted at a number of different temperatures in order to expand the data field, allowing for separation of enthalpy and free energy parameters. This type of experimental analysis makes no assumptions of optical linearity between the various heme groups and reveals that the triply ligated species is measurably significant for both human and bovine hemoglobin. It was also determined that the concentration of doubly ligated species of bovine hemoglobin is relatively low. The experiments indicate that the reactions for both hemoglobins are enthalpy-driven for oxygen stepwise additions 1, 2, and 4 while being entropy-driven for step 3. Human hemoglobin oxygen-binding experiments were also performed with the Gill thin-layer optical apparatus under solution conditions identical to those used in the calorimeter. The experiments revealed that if optical linearity is assumed, the overall third equilibrium constant is negative or near zero. This indicated that either the optical cell's performance is much poorer than the thin-layer calorimeter or there is an appreciable nonlinear optical effect.

Tetrameric hemoglobins have been at the center of inquiry into the nature of cooperativity and they continue to play a dominant role. These respiratory proteins are well suited for these studies due to rich spectra and convenient crystallographic and variegated functional characteristics. Our basic notions of allosteric (Koshland et al., 1966; Wyman, 1948, 1967), polysteric (Colosimo et al., 1976), and polyphasic (Wyman & Gill, 1980) molecular control through ligand-binding processes have their roots in the study of different species and mutants of hemoglobin. The literature pertinent to structure and function of heme proteins is vast and by virtue of its extent provides an unprecedented base upon which to test and extend our understanding of how these complex multisubunit proteins function in an optimum manner to extract oxygen from our environment. Reviews (Antonini & Brunori, 1971; Brunori et al., 1985; Rifkind, 1988) on general properties of heme proteins along with more detailed and recent accounts of structural properties (Baldwin & Chothia, 1979; Dickerson & Geis, 1983; Perutz, 1970, 1987) and functional studies (Ackers et al., 1992; Imai, 1982) provide a general overview of this field.

From a physiological point of view the key functional characteristics of respiratory proteins are represented by oxygen-binding curves and their dependence upon important regulatory ligands such as protons, carbon dioxide, organic phosphates, and chloride ions. Binding curves describe fundamental thermodynamic properties of ligand interactions with macromolecular systems (Wyman, 1964) and a full representation of the effects of one ligand on another are represented by linkage graphs (Wyman, 1984). The connection to molecular details is made by considerations of the relevant macromolecular species in the system. The description in terms of simple stoichiometric ligated species is given by the model of Adair (1925).

The critical test of any model is how well it represents a variety of functional information about a given system. The simultaneous effects of multiple ligand studies with $O_2$ and CO (Di Cera et al., 1987), $O_2$ and $CO_2$ (Doyle et al., 1987), and $O_2$ and organic phosphates (Robert et al., 1988) have provided critical information for examining the adequacy of molecular models. Likewise, where ligand linked dissociation occurs, as is present at low concentrations of hemoglobin, studies over a range of concentrations enable more accurate assessment of reaction parameters (Chu et al., 1984).

The accuracy of binding results is dependent upon the experimental method. Roughton et al. (1955) used gasometric methods. Spectroscopic methods based on the assumption of optical linearity with degree of saturation have been used in virtually all recent high-precision determinations (Ackers & Halvorson, 1974; Gill et al., 1987; Imai, 1982). Since similar binding-parameter results are found for different spectral regions, this has led to the conclusion that the determination of the parameters is free of any nonlinear effects between absorption and degree of saturation. Concerns have been raised over this assumption (Rifkin & Lumry, 1967), and indeed small nonlinear effects have been observed in various studies (Doyle et al., 1988; Imaizumi et al., 1978; Nasuda-Kouyama et al., 1983; Philo et al., 1981), but in general these effects have been regarded as having minor consequence on the determination of binding parameters for hemoglobin systems. However, a growing lack of agreement between the details of high-precision binding studies based on optical determinations—for example, the conclusion of very low triply ligated species in concentrated hemoglobin binding studies from this laboratory—has raised new concerns over the basic assumption of linear optical response. An initial study (Ownby & Gill, 1990) in the Soret region of $O_2$-$HbA_0$ in the presence of excess IHP[1] at 15 °C, conditions chosen to optimize sample

† This work was supported by NIH Grant HL22325 and NSF Grant DMB9004667.

‡ Deceased June 1991.

0006-2960/92/0431-10074$03.00/0 

Table I: Experimental Conditions

| species | buffer | reducing system |
|---|---|---|
| human hemoglobin $A_0$ | 4.75 mM heme<br>0.2 M potassium phosphate<br>1 mM EDTA<br>pH = 7.6 | 2.0 mM glucose 6-phosphate<br>10 μM catalase<br>10 μM ferredoxin<br>100 μM NADPH<br>100 μM glucose-6-phosphate dehydrogenase<br>1.0 μM ferredoxin-$NADP^+$ reductase |
| bovine hemoglobin $A_0$ | 4.43 mM heme<br>0.2 M potassium phosphate<br>1 mM EDTA<br>pH = 7.6 | 2.0 mM glucose 6-phosphate<br>10 μM catalase<br>10 μM ferredoxin<br>100 μM NADPH<br>100 μM glucose-6-phosphate dehydrogenase<br>1.0 μM ferredoxin-$NADP^+$ reductase |

stability, suggests that nonlinear effects are present and have the potential to distort parameter resolution in a serious way. It is important and crucial to explore this effect in greater detail. To this end we have developed a high-precision thin-layer gas-solution microcalorimeter which utilizes millimolar concentrations of heme in microliter quantities while exhibiting microjoule sensitivity. This method does not require any optical assumptions and is purely an enthalpic approach.

## MATERIALS AND METHODS

*General Preparations.* Human hemoglobin $A_0$ samples, stripped of organic phosphates, were prepared according to the method reported by Williams and Tsay (1973). Bovine hemoglobin samples in the absence of chloride were prepared on the basis of the method of Bare et al. (1975). The resulting hemoglobin, less than 3% met, was dialyzed at 6 °C for 36 h in three separate 6-L solutions of 0.2 M potassium phosphate and 1 mM EDTA at pH 7.6. The phosphate buffer was chosen for its small protonation heat of approximately −0.8 kcal/mol (Christensen et al., 1975). Purified protein samples were stored as pellets in liquid nitrogen until ready for use. The enzyme-reducing system of Hayashi et al. (1973) was used to reduce met formation (Table I); its components were purchased from Sigma and placed in the appropriate buffer before addition to the heme solutions. The samples were checked for alterations in pH before the experiment was begun.

Hemoglobin concentrations were determined using a previously calibrated thin-layer optical cell (0.0101 cm) placed in a Cary 219 spectrophotometer. Human hemoglobin extinction coefficients were taken from the values of Benesch et al. (1973) modified by Van Assendelft and Ziljstra (1975). A computer program based on these values was constructed to determine the concentrations of oxygenated and deoxygenated hemoglobin and methemoglobin components.[2] Bovine hemoglobin concentrations were determined using an extinction coefficient of $E = 0.868$ cm$^2$/mg for the carbonmonoxy derivative at 540 nm. Precise concentrations were determined to three significant figures after the addition of enzyme-reducing system just before the beginning of the experiment. Human and bovine hemoglobin concentrations were approximately 4.75 and 4.43 mM heme, respectively, with around 1% methemoglobin present when the enzyme system was sufficiently active. The samples were also removed and checked upon completion of the experiment and found to be less than 2% met. Bovine hemoglobin samples were monitored for met formation by exposing them to experimental conditions and checking for spectral absorbance decreases.

*Calorimetry.* The calorimeter has been described previously (Johnson et al., 1992). It consists of two aluminum blocks shielded by an aluminum case enclosed in a CPVC canister. Two thin-walled flat-bottom NMR tubes, acting as cell holders, extend through the top aluminum block into close-fitting copper cups mounted on thermophiles that are hooked in opposition (Twinned). The bottom aluminum block contains spring-loaded aluminum pistons serving to position the thermopiles with constant force against the copper cups, making it easier to assemble. Nominal 100-Ω resistor wires are wrapped around the outside of the copper cups and computer-controlled thermoelectrical compensation is employed. A stainless steel dilution valve at the top allows for the titration of gaseous ligands by way of successive logarithmic dilutions. The valve is equipped with an oxygen electrode in order to monitor the activity of oxygen and check the system for leaks. Temperature is controlled by a Tronac regulated water bath with deviations less than ±0.0003 °C.

The instrument is calibrated electrically by placing a nominal 100-Ω resistor wire wrapped around a thin-walled copper dowel inserted into an NMR tube cell. This cell, which mimics the sample orientation, is placed into the calorimeter, a series of calibration heats are run, and 0.43% heat loss is detected.

The sample and reference solutions, measured by Hamilton syringe (typically 50.0 μL), are suspended on a piece of filter paper that is placed on the inside wall of a flat-bottom modified NMR tube approximately 2.5 cm in length and 7 mm in diameter. These close-fitting cells are then inserted into the calorimeter so that they extend into the region of the copper cups.

The dilution valve operates by lowering the partial pressure of a reacting gas at constant temperature and pressure according to

$$P_i = P_0 D^i \quad (1)$$

$P_i$ is the partial pressure of a gas at dilution step $i$, $P_0$ is the starting pressure of the gas, and $D$ is the dilution factor of the valve. Experiments are conducted, in the case of oxygen binding to hemoglobin, by flushing the entire system with buffer-equilibrated compressed air. After the system is flushed, the bore of the valve is then turned toward the reaction and reference cells. The gas within the bore and cells is equilibrated to atmospheric pressure because the gas inlet is closed before the gas outlet. The bore is then turned so that it is disconnected from the cell and an inert gas such as nitrogen is allowed to fill the bore until the oxygen electrode indicates completion. The valve is then turned into the cell, the nitrogen is equilibrated to atmospheric pressure and the partial pressure of oxygen is diluted according to eq 1. Logarithmic reductions in oxygen partial pressures are made by repeating the above sequence until the reaction is complete. The dilution factor can be determined by fitting the partial pressure of oxygen indicated by the oxygen electrode versus the nitrogen dilution step number. The heat effect caused by the dissolution of gas is canceled out by the placement of enzyme system buffer in the reference cell. Reactions conducted with a number of different filter papers at varying concentrations of heme indicated no adverse filter paper interactions.

[1] Abbreviations: Hb, hemoglobin; EDTA, ethylenediaminetetraacetic acid; met, methemoglobin; IHP, inositol hexaphosphate; DPG, 2,3-diphosphoglycerate; CPVC, chlorinated poly(vinyl chloride).

[2] We thank Mauro Angeletti for the computer program used to determine hemoglobin concentration.

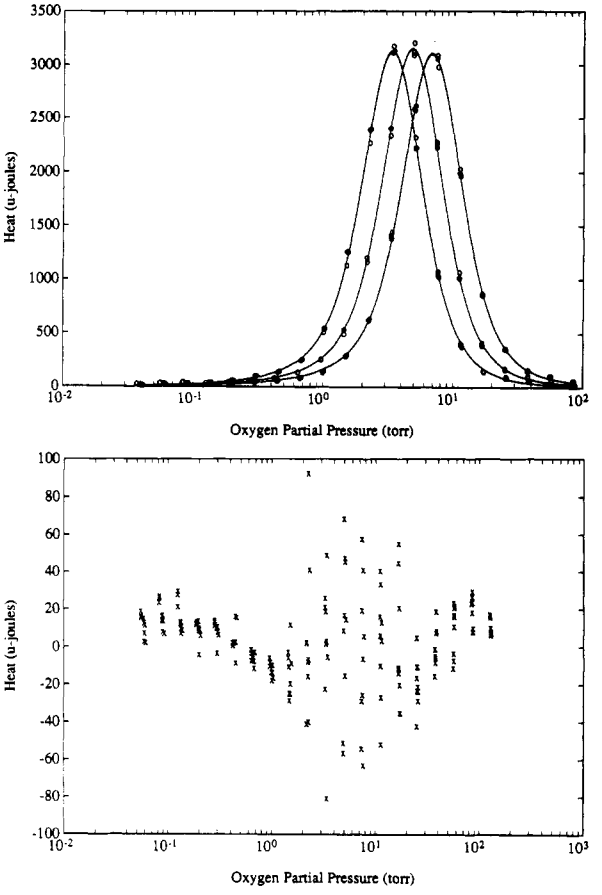


FIGURE 1: Three binding experiments performed for human hemoglobin at temperatures 15, 20, and 25 °C from left to right. Solid lines are plots of the fitted function and parameters at the appropriate temperatures and ligand activities. (Top) Human hemoglobin data and fitted function. (Bottom) Residuals show the greatest errors in the middle of the binding curve due to longer compensation times and higher heats.

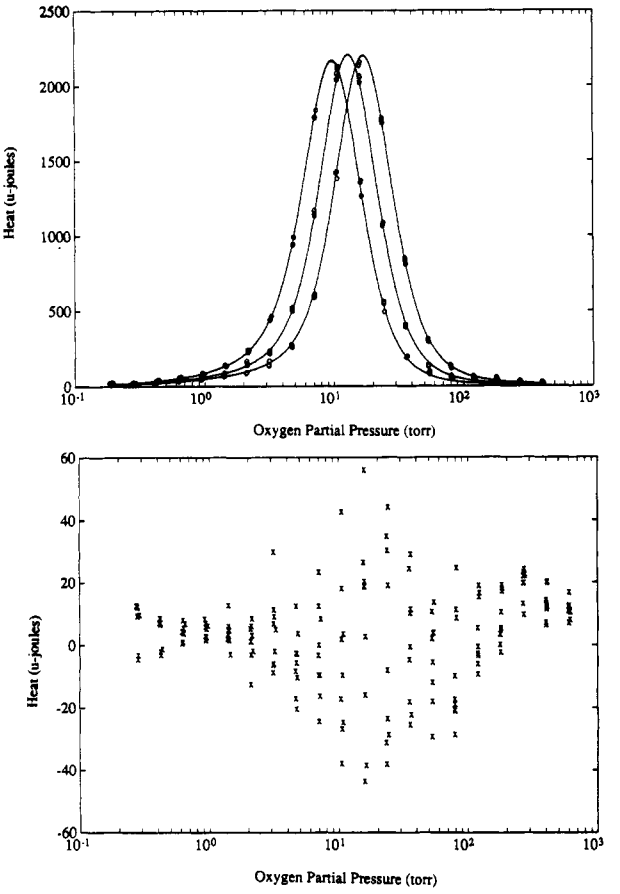


FIGURE 2: Three binding experiments performed for bovine hemoglobin at temperatures 15, 20, 25 °C from left to right. Solid lines are plots of the fitted function and parameters at the appropriate temperatures. (Top) Bovine hemoglobin data and fitted function. (Bottom) Residuals.

*Thin-Layer Optical Apparatus.* Optical binding data were obtained with the Gill thin-layer apparatus (Doleman & Gill, 1978) which has been subjected to a number of alterations over the last 15 years. In this method a thin layer of sample approximately 0.002 in. thick is suspended between an optical window and a gas-permeable membrane. This is accomplished by placing the sample in a cubical cell that can be removed from the gas-dilution portion of the apparatus. Sample thickness is controlled by the use of a stainless steel shim inserted between the optical window and membrane. The gas-permeable membrane is in direct contact with the gas reservoir that is controlled by the dilution valve. Temperature is controlled by a Lauda circulating water bath. A quartz thermometer has been retrofitted to the valve assembly so that the temperature can be controlled to a few hundredths of a degree Celsius.

Experiments are conducted by first flushing the entire system with buffer-equilibrated oxygen or air until equilibrium is reached. The sample is then titrated by lowering the partial pressure of oxygen with nitrogen and noting the absorbance decrease at 576 nm as oxygen is released from the hemoglobin. Absorbance changes are detected by the placement of the thin-layer apparatus into a Cary 219 spectrophotometer. Titration is accomplished by the use of a precision dilution valve in which the bore of the valve is flushed with nitrogen and released into the reaction cell in a stepwise manner. The stepwise addition of nitrogen, as with the calorimeter, serves to lower the oxygen partial pressure logarithmically. The operation of the thin-layer optical cell is analogous to that of the thin-layer microcalorimeter in that the partial pressure of gaseous reacting ligand is lowered in a precise logarithmic fashion. The major difference between the instruments lies in their detection principles. The optical cell measures absorbance changes while the thin-layer calorimeter detects enthalpy changes.

*Data Analysis.* The experiments conducted in this paper are ideally suited for analysis utilizing equilibrium and enthalpy expressions defined in the Adair formalism. Gill thin-layer optical binding data (Doleman & Gill, 1976) are taken in the form of absorbance changes for a given change in partial pressure of oxygen. Analogously, calorimetric heat binding data are taken as enthalpy changes for a change in oxygen partial pressure. In order to fit these types of data, the Adair representation (Adair, 1925) is utilized to generate expressions that are similar to each other. We begin by depicting the four-site oxygen-binding hemoglobin system by the following series of equilibria:

$$Hb + O_2 \leftrightarrow HbO_2 \quad \Delta H_1, \beta_1 \tag{2}$$

$$Hb + 2O_2 \leftrightarrow Hb(O_2)_2 \quad \Delta H_2, \beta_2 \tag{3}$$

$$Hb + 3O_2 \leftrightarrow Hb(O_2)_3 \quad \Delta H_3, \beta_3 \tag{4}$$

$$Hb + 4O_2 \leftrightarrow Hb(O_2)_4 \quad \Delta H_4, \beta_4 \tag{5}$$

The $\Delta H$'s and $\beta$'s are the overall enthalpies and equilibrium constants, respectively, for the given expressions. The average enthalpy of a macromolecule and the degree of ligand

Table II: Calorimetric Cross-Correlation Matrix for the Overall Adair Constants and Enthalpies of Human Hemoglobin

| | $H_1$ | $H_2$ | $H_3$ | $H_4$ | $\beta_1$ | $\beta_2$ | $\beta_3$ | $\beta_4$ |
|---|---|---|---|---|---|---|---|---|
| $H_1$ | 1.000 | | | | | | | |
| $H_2$ | −0.0921 | 1.000 | | | | | | |
| $H_3$ | 0.0572 | −0.4561 | 1.000 | | | | | |
| $H_4$ | 0.5479 | 0.1685 | 0.2812 | 1.000 | | | | |
| $\beta_1$ | 0.3421 | −0.0274 | −0.5251 | −0.2647 | 1.000 | | | |
| $\beta_2$ | 0.1581 | 0.5416 | 0.3934 | 0.5447 | −0.5603 | 1.000 | | |
| $\beta_3$ | −0.0926 | −0.2267 | −0.6499 | −0.5811 | 0.6561 | 0.9092 | 1.000 | |
| $\beta_4$ | 0.4887 | 0.2684 | 0.0081 | 0.2199 | 0.6350 | 0.1929 | −0.1081 | 1.000 |

Table III: Calorimetric Cross-Correlation Matrix for the Overall Adair Constants and Enthalpies of Bovine Hemoglobin

| | $H_1$ | $H_2$ | $H_3$ | $H_4$ | $\beta_1$ | $\beta_2$ | $\beta_3$ | $\beta_4$ |
|---|---|---|---|---|---|---|---|---|
| $H_1$ | 1.000 | | | | | | | |
| $H_2$ | 0.5715 | 1.000 | | | | | | |
| $H_3$ | 0.2291 | 0.7842 | 1.000 | | | | | |
| $H_4$ | 0.5445 | 0.4390 | 0.3230 | 1.000 | | | | |
| $\beta_1$ | 0.6596 | −.0236 | −0.2444 | 0.0480 | 1.000 | | | |
| $\beta_2$ | 0.5408 | 0.9885 | 0.8333 | 0.4501 | −0.0816 | 1.000 | | |
| $\beta_3$ | −0.3203 | −0.8765 | −0.9041 | −0.4670 | 0.2098 | −0.9148 | 1.000 | |
| $\beta_4$ | 0.7686 | 0.2838 | 0.1107 | 0.2026 | 0.9307 | 0.2336 | −0.1247 | 1.000 |

Table IV: Calorimetric Table of Parameters for Human Hemoglobin

| parameter | value | simulation errors |
|---|---|---|
| $B_1$ (Torr$^{-1}$) | 0.093 | ±0.013 |
| $B_2$ (Torr$^{-2}$) | 0.0081 | ±0.0010 |
| $B_3$ (Torr$^{-3}$) | 0.00049 | ±0.000090 |
| $B_4$ (Torr$^{-4}$) | 0.000311 | ±0.000018 |
| $\Delta H_1$ (kcal/mol) | −10.3 | ±1.1 |
| $\Delta H_2$ (kcal/mol) | −27.1 | ±1.7 |
| $\Delta H_3$ (kcal/mol) | −27.8 | ±4.3 |
| $\Delta H_4$ (kcal/mol) | −48.1 | ±0.14 |

Table V: Calorimetric Table of Parameters for Bovine Hemoglobin

| parameter | value | simulation errors |
|---|---|---|
| $B_1$ (Torr$^{-1}$) | 0.071 | ±0.010 |
| $B_2$ (Torr$^{-2}$) | 0.00027 | ±0.00012 |
| $B_3$ (Torr$^{-3}$) | 0.000046 | ±0.0000072 |
| $B_4$ (Torr$^{-4}$) | 0.0000108 | ±0.0000012 |
| $\Delta H_1$ (kcal/mol) | −6.7 | ±0.68 |
| $\Delta H_2$ (kcal/mol) | −38.5 | ±4.7 |
| $\Delta H_3$ (kcal/mol) | −18.3 | ±3.9 |
| $\Delta H_4$ (kcal/mol) | −35.2 | ±0.12 |

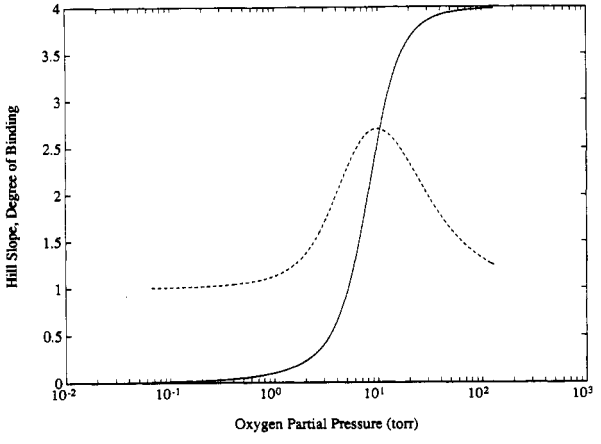


FIGURE 3: Maximum Hill slope for human hemoglobin is 2.7; the $P_m$ is 7.53 Torr at 25 °C.

saturation can be treated in a parallel manner in a general statistical mechanical framework (Gill et al., 1985). The hemoglobin oxygen-binding macromolecular system can be described in terms of the populations of its various ligated free energy levels (Wyman, 1967). The binding partition

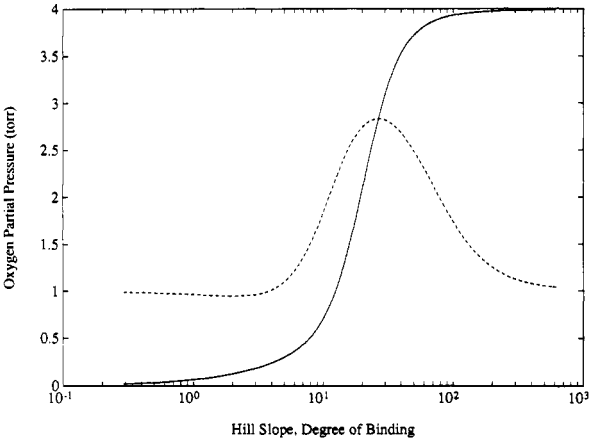


FIGURE 4: Maximum Hill slope for bovine hemoglobin is 2.83; the $P_m$ is 17.5 Torr at 25 °C.

function or binding polynomial $P$, which is the sum of these states, can be expressed, taking the unligated macromolecule as the reference state, in terms of the above equilibrium constants $\beta$ and the ligand activity $x$:

$$P = 1 + \beta_1 x + \beta_2 x^2 + \beta_3 x^3 + \beta_4 x^4 \quad (6)$$

This binding polynomial in the Adair formalism is a function of the ligand activity and temperature. The temperature dependence of the overall binding constants $\beta_j$ is given in terms of the overall enthalpies $\Delta H_j$ and the gas constant $R$:

$$\frac{\partial \ln \beta_j}{\partial 1/T} = -\frac{\Delta H_j}{R} \quad (7)$$

The partition function or binding polynomial formalism allows for the generation of expressions for the fractional saturation $\theta$ and the average enthalpy $H$ (relative to the reference state $H_0$) by taking the appropriate derivatives of $P$:

$$\theta = \frac{1}{4}\left(\frac{\partial \ln P}{\partial \ln x}\right)_T \quad (8)$$

$$\bar{H} - \bar{H}_0 = -R\left(\frac{\partial \ln P}{\partial (1/T)}\right)_x \quad (9)$$

Equation 8 describing the fractional saturation has been used in a number of optical studies (Gill et al., 1987; Parody-Morreale et al., 1987; Bucci et al., 1991). In this paper we

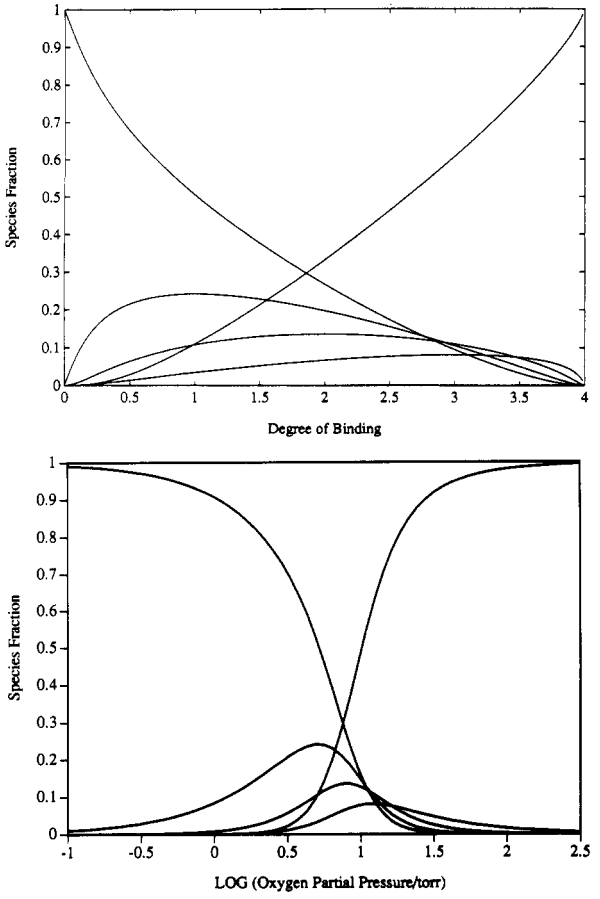


FIGURE 5: Species fraction plot for human hemoglobin, revealing significant triply ligated species.

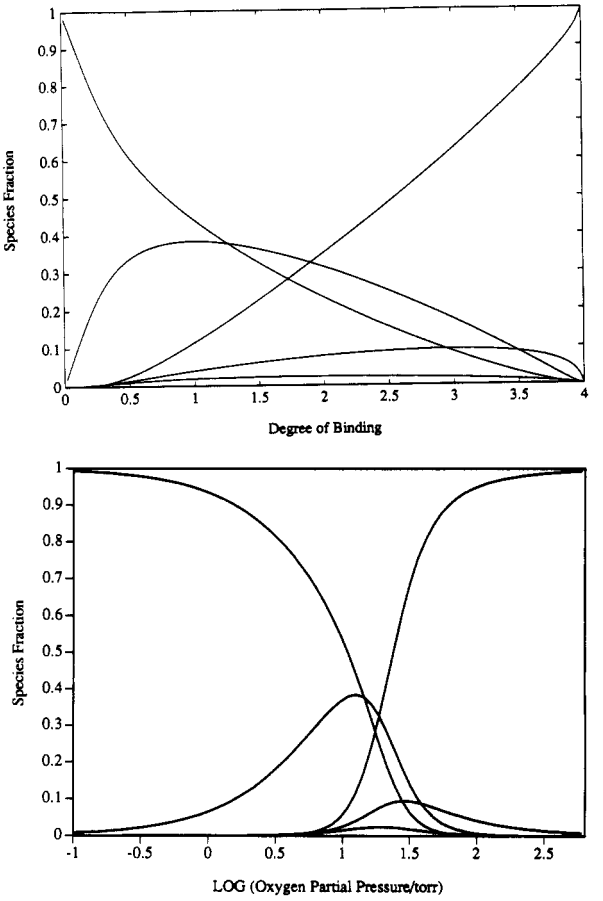


FIGURE 6: Species fraction plot for bovine hemoglobin, revealing significant triply ligated species with relatively low concentration of doubly ligated species.

will develop both the optical and enthalpy expressions in order to describe oxygen binding to hemoglobin, first assuming optical linear linearity and then from a purely thermodynamic perspective. The optical expression for the four sites of hemoglobin after differentiation is

$$\theta = \frac{\beta_1 x + 2\beta_2 x^2 + 3\beta_3 x^3 + 4\beta_4 x^4}{4(1 + \beta_1 x + \beta_2 x^2 + \beta_3 x^3 + \beta_{4x}{}^4)} \tag{10}$$

The analogous enthalpy expression for the four oxygen sites of hemoglobin is

$$\bar{H} - \bar{H}_0 = \frac{\Delta\bar{H}_1\beta_1 x + \Delta\bar{H}_2\beta_2 x^2 + (\Delta\bar{H}_3)\beta_3 x^3 + (\Delta\bar{H}_4)\beta_4 x^4}{1 + \beta_1 x + \beta_2 x^2 + \beta_3 x^4 + \beta_{4x}{}^4} \tag{11}$$

The experiments conducted with the instruments described above yield differential optical and heat binding curves in which the absorbance and enthalpy changes for a given oxygen partial pressure change are monitored. The theoretical reaction absorbances and enthalpies for these types of experiments are given by

$$(\Delta OD_i)^{theor} = (\theta_i - \theta_{i-1})\Delta OD_T \tag{12}$$

$$q_i{}^{theor} = [(\bar{H} - \bar{H}_0)_i - (\bar{H} - \bar{H}_0)_{i-1}]C_{Hb}V \tag{13}$$

Here $(\Delta OD_i)^{theor}$ is the calculated optical density change at step $i$ and $\Delta OD_T$ is the total optical density change. $q_i{}^{theor}$ is the calculated heat at step $i$, $C_{Hb}$ is the molar concentration of hemoglobin, and $V$ is the volume of the solution in liters. Binding parameters are estimated by least-squares optimization using the Marquardt algorithm in which the experimentally measured optical density changes and enthalpies can be compared with the theoretically calculated optical density changes and enthalpies and the standard deviation of the fit computed:

$$\sigma^2 = \frac{\sum_k \sum_i (\Delta OD_i{}^{exp} - \Delta OD_i{}^{theor})^2}{\nu} \tag{14}$$

$$\sigma^2 = \frac{\sum_k \sum_i (q_i{}^{exp} - q_i{}^{theor})^2}{\nu} \tag{15}$$

The additional summation $k$ is added to allow for multiple data sets and $\nu$ is the number of degrees of freedom. The standard error of a point (SEP) gives a measure of the adequacy of the fit and is defined as the square root of the standard deviation. Parameter errors at the 67% confidence level are determined by use of the linear approximation of the curvature matrix (Bevington, 1969). The "true errors" (67% confidence level) are estimated by generating a series of 500 complete optical or calorimetric binding-curve data sets using parameter values corresponding to those of the experiments. Each generated data set is given pseudorandom errors (consistent with the SEP) following a Gaussian distribution indicative of the experimental residuals. These simulations are individually fitted and the average parameter errors are computed. This method of error analysis gives an indication of what the "true errors" would be if one could conduct the experiment a large number of times.

Initially, single-temperature optical binding curves were fit to determine the Adair constants in order to confirm previous

Table VI: Intrinsic Human Stepwise Thermodynamics at 25 °C[a]

| | $Hb + O_2 \leftrightarrow HbO_2$ | $HbO_2 + O_2 \leftrightarrow Hb(O_2)_2$ | $Hb(O_2)_2 + O_2 \leftrightarrow Hb(O_2)_3$ | $Hb(O_2)_3 + O_2 \leftrightarrow Hb(O_2)_4$ |
|---|---|---|---|---|
| $\Delta H$ (kcal/mol) | −10.3 ± 1.1 | −16.8 ± 2.0 | −0.7 ± 4.6 | −20.3 ± 4.3 |
| $\Delta G$ (kcal/mol) | −5.7 ± 0.1 | −6.2 ± 0.2 | −6.5 ± 0.2 | −8.5 ± 0.1 |
| $\Delta S$ [cal/(mol·deg)] | −15.4 ± 3.7 | −35.6 ± 6.7 | +19.5 ± 15.4 | −39.6 ± 14.4 |
| $T\Delta S$ (kcal/mol) | −4.6 ± 1.1 | −10.6 ± 2.0 | +5.8 ± 4.6 | −11.8 ± 4.3 |

[a] All reactant and product concentrations are specified as molar in aqueous solution using 1.613 μM/Torr for the oxygen solubility at 25 °C (Kilmartin et al. 1978).

Table VII: Intrinsic Bovine Stepwise Thermodynamics at 25 °C[a]

| | $Hb + O_2 \leftrightarrow HbO_2$ | $HbO_2 + O_2 \leftrightarrow Hb(O_2)_2$) | $Hb(O_2)_2 + O_2 \leftrightarrow Hb(O_2)_3$ | $Hb(O_2)_3 + O_2 \leftrightarrow Hb(O_2)_4$ |
|---|---|---|---|---|
| $\Delta H$ (kcal/mol) | −6.7 ± 0.7 | −31.8 ± 4.7 | +20.2 ± 6.1 | −17.0 ± 3.9 |
| $\Delta G$ (kcal/mol) | −5.5 ± 0.1 | −4.4 ± 0.2 | −7.1 ± 0.3 | −7.9 ± 0.1 |
| $\Delta S$ [cal/(mol·deg)] | −4.0 ± 2.4 | −91.9 ● 15.8 | +91.6 ± 20.5 | −30.5 ± 13.1 |
| $T\Delta S$ (kcal/mol) | −1.2 ± 0.7 | −27.4 ± 4.7 | +27.3 ± 6.1 | −9.1 ± 3.9 |

[a] All reactant and product concentrations are specified as molar in aqueous solution using 1.613 μM/Torr for the oxygen solubility at 25 °C (Kilmartin et al., 1978).

work (Gill et al., 1987). Next, the enthalpies of ligation and equilibrium constants were fit from optical binding curves at a series of temperatures by combining eqs 7 and 10. This van't Hoff study was conducted in an attempt to verify the information obtained from the calorimeter. The calorimetric data was initially fit at one temperature but the eight parameters proved to be too highly correlated to be separated. As with the optical data, the equilibrium constants are found to depend greatly on temperature (eq 7); therefore, as before, the data field was expanded by conducting experiments at a number of different temperatures.

## RESULTS

In this study the buffer and enzyme-reducing system components are carefully controlled to eliminate the side effects shown to exist in a previous paper (Johnson et al., 1992). Experiments performed without the enzyme system at 15 °C did not differ significantly from those with the enzyme system present. Higher temperatures require the use of enzymes as met formation is evident over the course of the experiment. Solution conditions (Table I) are chosen to minimize the heat of protonation of the buffer by the release of Bohr protons as well as the formation of dimers.

*Calorimetric Data.* Three sets of three heat binding curve experiments were conducted with both human and bovine hemoglobin at 15, 20, and 25 °C (Figures 1 and 2, top panels). A global computer analysis was performed on all the data sets for each species and the fits are shown in Figures 1 and 2, top panels, the standard error of a point being 23.7 μJ for human and 16.3 μJ for bovine, which is reasonable for this type of instrument. The corresponding residuals are given in Figures 1 and 2, bottom panels. The residuals display the greatest errors near the middle of the binding curve, which is consistent with the higher heats and longer compensation times in this region. The parameter cross-correlation matrices (Tables II and III) revealed little parameter dependence, with the exception of the bovine $\beta_2$ and $H_2$, where the low value of the doubly ligated species increases the correlation (Magar, 1972). In fact, Johnson et al. (1976) have shown that a fitting parameter can be solved from reasonably precise data if the pertinent cross-correlation coefficients are less than 0.98 (absolute value); only one of the cross-correlation coefficients exceeds 0.98. Errors were estimated by generating a series of 500 complete heat binding curve sets using parameter values corresponding to those of the experiments. To each generated data set pseudorandom errors were added following a Gaussian

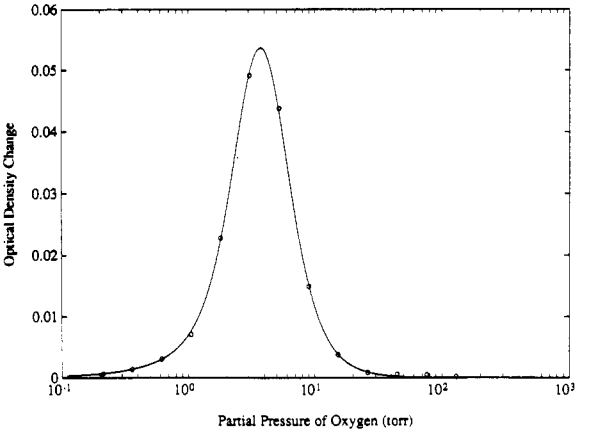


FIGURE 7: Typical nonlinear least-squares fit of a single isothermal optical binding curve of human hemoglobin at 10 °C. Results for isothermal optical fits at 5, 10, 15, 20, and 25 °C are shown in Table VIII.

distribution. The resulting errors, obtained by fitting these simulations, are given in Tables IV and V, along with the values of the parameters obtained from experiment. The maximum Hill slope for human hemoglobin, Figure 3, is 2.7; the $P_m$ at 25 °C is 7.53 Torr and the Hill slope at the $P_m$ is 2.63. The maximum Hill slope for bovine hemoglobin, Figure 4, is 2.83; the $P_m$ at 25 °C is 17.5 Torr and the Hill slope at the $P_m$ is 2.64. The species fraction plots, Figures 5 and 6, indicate the presence of significant triply ligated species for both human and bovine hemoglobins. Bovine hemoglobin, however, does exhibit a relatively low doubly ligated species. The intrinsic stepwise thermodynamic breakdown is given in Tables VI and VII.

*Optical Data.* Optical binding experiments conducted in duplicate were performed with human hemoglobin under solution conditions identical to those in the heat binding studies. The temperature range for these experiments was from 5 to 25 °C in 5 °C increments. Single isothermal binding curves were initially fit in an attempt to obtain the Adair coefficients. As expected, the third overall equilibrium constants were found to be negative or statistically near zero (Figure 7, Table VIII). One useful aspect of this fitting procedure was the calculation of the median activity ($P_m$). The $P_m$'s were found to be within a few hundredths of a torr of their heat binding counterparts (Table VIII). This indicated that the gas dilution method in the optical cell was, from an overall standpoint, similar to the calorimetric method. A global computer analysis was performed on all of the data sets in an attempt to reveal the

Table VIII: Human Hemoglobin Optical Parameters (Isothermal Fitting)

| parameter | temperature | | | | |
|---|---|---|---|---|---|
| | 5.0 °C | 10.0 °C | 15.0 °C | 20.0 °C | 25.0 °C |
| $\beta_1$ (Torr$^{-1}$) | 0.243 ± 0.098 | 0.171 ± 0.076 | 0.123 ± 0.041 | 0.0615 ± 0.0168 | 0.0581 ± 0.0145 |
| $\beta_2$ (Torr$^{-2}$) | 0.165 ± 0.056 | 0.0956 ± 0.029 | 0.0408 ± 0.011 | 0.0242 ± 0.0033 | 0.0149 ± 0.0019 |
| $\beta_3$ (Torr$^{-3}$) | −0.0009 ± 0.026 | −0.0057 ± 0.0091 | −0.0049 ± 0.0024 | −0.0011 ± 0.0005 | −0.0004 ± 0.00023 |
| $\beta_4$ (Torr$^{-4}$) | 0.101 ± 0.0071 | 0.0226 ± 0.0018 | 0.00530 ± 0.0003 | 0.00123 ± 0.00004 | 0.000310 ± 0.000015 |
| $\Delta OD_{tot}$ | 0.201 ± 0.0021 | 0.149 ± 0.0018 | 0.214 ± 0.0020 | 0.190 ± 0.0011 | 0.1417 ± 0.0010 |
| $P_m$ (Torr) | 1.77 | 2.58 | 3.70 | 5.39 | 7.52 |
| heat binding $P_m$ (Torr) | 1.74 | 2.56 | 3.72 | 5.33 | 7.53 |

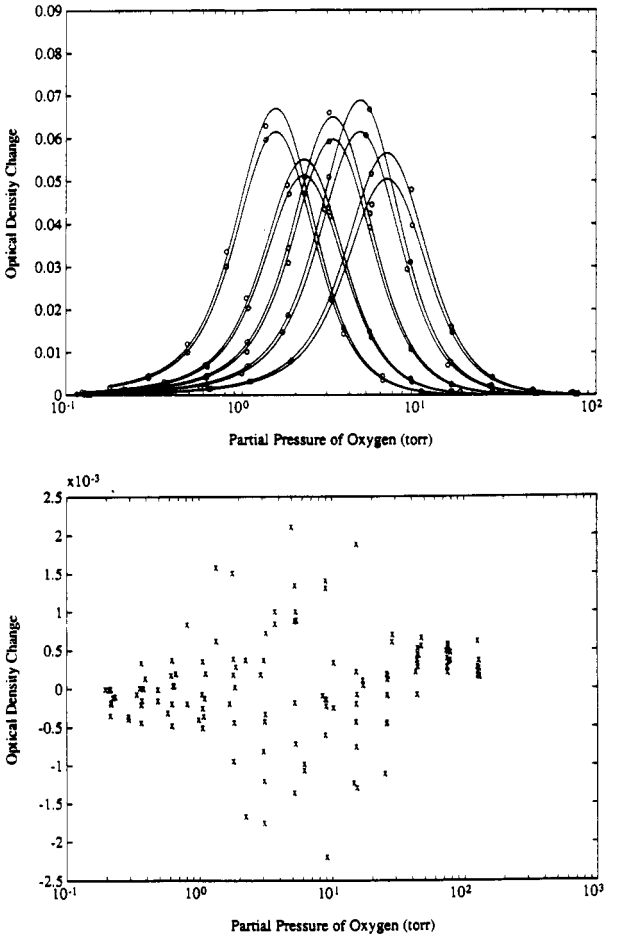


FIGURE 8: Two optical binding curves experiments performed for human hemoglobin at each of the temperatures 5, 10, 15, 20, and 25 °C from left to right. Solid lines are plots of the fitted function and parameters at the appropriate temperatures and ligand activities. Note that layer thickness is difficult to control, resulting in various total optical density changes. (Top) Human hemoglobin data and fitted function. (Bottom) Residues show the greatest errors in the middle of the binding curve due to longer baseline equilibration times and larger optical density changes.

Table IX: Optical Table of Parameters for Human Hemoglobin

| parameter | value | simulation errors |
|---|---|---|
| $\beta_1$ (Torr$^{-1}$) | 0.053 | ±0.012 |
| $\beta_2$ (Torr$^{-2}$) | 0.012 | ±0.0019 |
| $\beta_3$ (Torr$^{-3}$) | −0.00041 | ±0.00020 |
| $\beta_4$ (Torr$^{-4}$) | 0.000297 | ±0.000018 |
| $\Delta H_1$ (kcal/mol) | −13.1 | ±3.5 |
| $\Delta H_2$ (kcal/mol) | −22.9 | ±2.5 |
| $\Delta H_3$ (kcal/mol) | −36.3 | ±7.1 |
| $\Delta H_4$ (kcal/mol) | −48.4 | ±0.9 |

overall enthalpy values as well as the Adair binding constants (Figure 8, Table IX). As before, the errors (67% confidence level) were estimated by generating a series of 500 complete optical binding curve sets using parameter values corresponding to those of the experiments. To each generated data set were added pseudorandom errors, following a Gaussian distribution that corresponded closely with the residuals. The resulting errors obtained by performing these simulations are given in Table IX along with the values of the parameters obtained from experiment (species fraction plot Figure 9). The parameter cross-correlation matrix (Table X) reveals little parameter dependence. It is evident that the optically obtained parameter values are statistically different from those obtained by heat binding curve analysis. In fact, the appearance of a negative overall triply ligated equilibrium constant suggests a flaw in the optical determination; either the optical cell's performance is much poorer than the thin-layer calorimeter or there is an appreciable nonlinear optical effect.

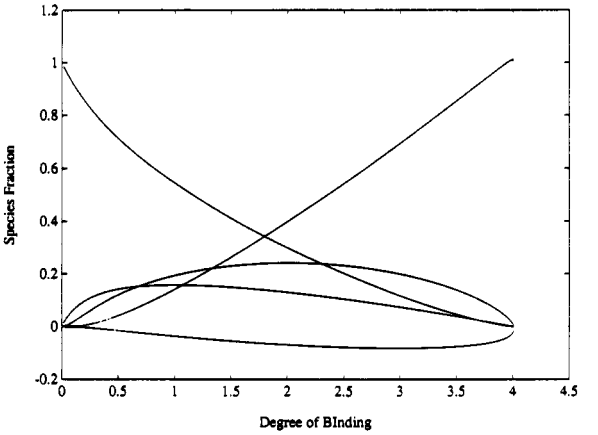


FIGURE 9: Species fraction plot of parameters from Table IX, revealing the implausible featuring of a negative $\beta_3$ value.

## DISCUSSION

Over the last few years our laboratory as well as others have utilized the Gill thin-layer optical dilution apparatus (Doleman & Gill, 1976) to determine the binding constants of hemoglobin under a number of different solution conditions. At physiological pH the overall equilibrium constant $\beta_3$ is found to be very low or uncertain, requiring it to be fixed at values greater than zero to obtain a somewhat meaningful fit of the data (Gill et al., 1987; Vandegriff et al., 1989). Ownby and Gill (1990) have shown that this may be due to the nonlinear optical properties associated with differences between the four heme sites. In the present series of calorimetric experiments, for both human and bovine hemoglobin, $\beta_3$ is found to be positive and in fact larger than $\beta_4$ at 25 °C. These findings support the proposal of Ownby and Gill (1990) that the origin of a zero value for $\beta_3$ lies in a nonlinear optical response of $O_2$ binding to hemoglobin, which distorts the parameter resolution of the optical binding curve.

The conditions for the present experiments, pH 7.6, 0.2 M potassium phosphate, and 1 mM EDTA, were chosen to minimize the heterotropic modulation of $O_2$ binding by chloride and DPG. The buffer, potassium phosphate, was selected to

Table X: Optical Cross-Correlation Matrix for the Overall Adair Constants and Enthalpies of Human Hemoglobin

| | $H_1$ | $H_2$ | $H_3$ | $H_4$ | $\beta_1$ | $\beta_2$ | $\beta_3$ | $\beta_4$ |
|---|---|---|---|---|---|---|---|---|
| $H_1$ | 1.000 | | | | | | | |
| $H_2$ | –0.6337 | 1.000 | | | | | | |
| $H_3$ | 0.3444 | –0.9211 | 1.000 | | | | | |
| $H_4$ | 0.5381 | 0.2789 | 0.5810 | 1.000 | | | | |
| $\beta_1$ | 0.8104 | –0.4848 | –0.2911 | –0.4078 | 1.000 | | | |
| $\beta_2$ | 0.5170 | 0.7790 | 0.7626 | 0.2516 | –0.6442 | 1.000 | | |
| $\beta_3$ | –0.2878 | –0.7120 | –0.8090 | –0.4714 | 0.3855 | –0.9344 | 1.000 | |
| $\beta_4$ | 0.4303 | 0.2430 | 0.4891 | 0.8160 | 0.4947 | 0.3179 | –0.5861 | 1.000 |

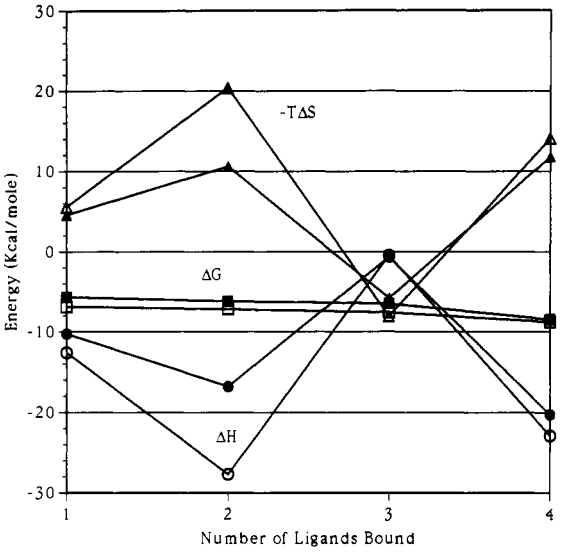


FIGURE 10: Thermodynamic parameters for the intrinsic stepwise oxygenation of human hemoglobin at pH 9.0, borate buffer, determined optically (open symbols) (Bucci et al., 1991). Calorimetric values are shown with dark symbols.

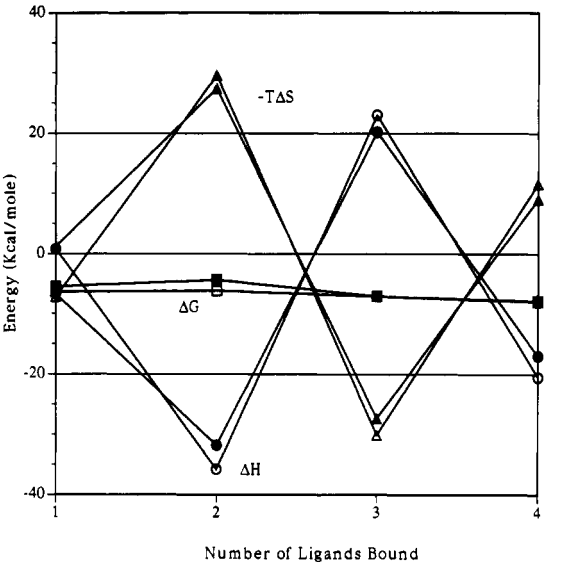


FIGURE 11: Thermodynamic parameters for the intrinsic stepwise oxygenation of bovine hemoglobin at pH 9.0, determined optically (open symbols) (Bucci et al., 1991). Calorimetric values are shown with dark symbols.

minimize the contribution of the heat of protonation of the buffer to the enthalpy changes for the system. To our knowledge there have been no studies which determine the enthalpy–entropy partitioning for each step of $O_2$ binding under these exact conditions and thus comparison with other studies must be made with caution.

In a previous paper (Johnson et al., 1992), the overall binding of oxygen as well as carbon monoxide to horse and sperm whale myoglobin and human hemoglobin were examined. The binding of oxygen is shown to be an exothermic event and it is reasonable to assume that this enthalpy is the primary driving force of binding. As pointed out by Bucci et al. (1991), however, the situation is much more complicated for human hemoglobin in that the heat release is reversed upon the third ligation step. It appears that the addition of a third oxygen is an entropy-driven reaction while the others are enthalpy-driven (Table VI). The first and third stepwise oxygen-binding steps yield enthalpy values of $-10.3 \pm 1.1$ and $0.7 \pm 4.6$ kcal/mol of heme, respectively. This is less exothermic than the noncooperative oxygen binding to myoglobin, $-16.0 \pm 0.05$ kcal/mol of heme. These lower values may be attributed to conformational protein changes (Chothia, 1974), changes in salt bridges, and changes in the state of protonation (Perutz, 1970). The second and fourth stepwise additions have enthalpies of $-16.8 \pm 2.0$ and $-20.3 \pm 4.3$ kcal/mol of heme, respectively. These values are close to the intrinsic value of myoglobin, with the excess possibly due to greater exposure of hydrophobic residues on the surface following a conformation change.

In order to further investigate and clarify the extreme entropy–enthalpy compensation taking place as successive ligands of oxygen are bound, we have compared the values obtained by Bucci et al. (1991) at pH 9.0 with our values obtained at pH 7.6. This procedure is carried out while recognizing that hemoglobin is very sensitive to its environment, exhibiting drastic changes in affinity when exposed to a number of allosteric effectors and buffer conditions. A qualitative comparison of the first four stepwise enthalpy values obtained for human hemoglobin by Bucci et al. at pH 9.0 (Figure 10) with those obtained from our set of calorimetric experiments (Table VI) reveals the major difference is found in the second stepwise reaction. This difference, in which the enthalpy value at pH 7.6 is less exothermic than at pH 9.0, is probably explained by the Bohr effect (Perutz, 1970). As detailed previously (Johnson et al., 1992), the Bohr effect at pH 7.6 increases the non-Bohr-associated enthalpy by approximately 4.5 kcal/mol of heme (due to the deprotonation of amino acid residues such as histidine).

Comparison of the bovine hemoglobin stepwise thermodynamic values (Table VII) reveals there is little difference between the two. If the assumption is made that borate and phosphate have similar effects on the molecule, one could conclude that the bovine Bohr effect at pH 7.6 is similar to that at pH 9.0. Bovine data by Fronticelli et al. (1990) between pH values 7.6 and 8.1 reveals little hydrogen ion Bohr effect. The maximum effect is displayed betwen pH 6.7 and 7.3, tailing off as the pH is increased. If the bovine hemoglobin Bohr effect behaves in the same manner as human, then the extrapolation to pH 9.0 would still reveal little Bohr effect. This would be consistent with our findings.

In light of the disagreement between the thermodynamic parameters obtained by calorimetric and optical methods at pH 7.6 (Tables IV and IX), the question arises as to why there

is good general agreement between the thermodynamic parameters determined by the calorimetric method at pH 7.6 and by the optical method at pH 9.0 (Bucci et al., 1991) (Figures 10 and 11) once the Bohr effect is taken into account. It is known that increasing the pH of hemoglobin solutions decreases the cooperativity, resulting in higher concentrations of intermediate species. Simulations indicate that increased intermediate populations make it possible to resolve the thermodynamic parameters under conditions of greater error. Thus nonlinear optical effects or instrumental uncertainties resulting in increased error may very well be negligible under these conditions.

At this point it would be difficult to speculate on the exact mechanism for oxygen binding and heat release in human hemoglobin. However, given the nature of the enthalpy–entropy compensation for each ligand-binding reaction, it appears likely that there are more than two specific conformational states in the T to R transition, with the major modulation occuring at the third ligation step.

## REFERENCES


Ackers, G. K., & Halvorson, H. R. (1974) *Proc. Natl. Acad. Sci. U.S.A. 71*, 4312.

Ackers, G. K., Doyle, M. L., Meyers, D., & Dougherty, M. A. (1992) *Science 255*, 54.

Adair, G. S. (1925) *Proc. R. Soc. London, B: Biol. Sci. A109*, 292.

Antonini, E., & Brunori, M. (1971) *Hemoglobin and Myoglobin in their Reactions with Ligands*, Frontiers in Biology, North Holland Publishing, Amsterdam.

Baldwin, J., & Chothia, C. (1979) *J. Mol. Biol. 129*, 175.

Bare, G. H., Alben, J. O., & Bromberg, P. A. (1975) *Biochemistry 14*, 1578.

Benesch, R. E., Benesch, R., & Yung, S. (1973) *Anal. Biochem. 55*, 245.

Bevington, P. (1969) *Data Reduction and Error Analysis for the Physical Sciences*, McGraw-Hill, New York.

Bucci, E., Fronticelli, C., & Gryczynski, Z. (1991) *Biochemistry 30*, 3195.

Brunori, M., Coletta, M., & Giardina (1985) *Metalloproteins: Part 2: Metal Proteins with Non-redox Roles* (Harrison, P. M., Ed.) p 263, Macmillan Press, London.

Christensen, J. J., Hansen, L. D., & Izatt, R. M. (1975) *Handbook for Proton Ionization Heats and Related Thermodynamic Quantities*, Wiley and Sons, New York.

Chu, A., Turner, B. W., & Ackers, G. K. (1984) *Biochemistry 23*, 604.

Chothia, C. (1974) *Nature 248*, 330.

Colosimo, A., Brunori, M., & Wyman, J. (1974) *Biophys. Chem. 2*, 338.

DiCera, E., Doyle, M. L., Connelly, P. R., & Gill, S. J. (1987) *Biochemistry 26*, 6494.

Dickerson, R. E., & Geis, I. (1983) *Hemoglobin*, Benjamin/Cummings, Menlo Park, CA.

Doleman, D., & Gill, S. J. (1976) *Anal. Biochem. 87*, 127.

Doyle, M. L., Di Cera, E., Robert, C. H., & Gill, S. J. (1987) *J. Mol. Biol. 196*, 927.

Doyle, M. L., DiCera, E., & Gill, S. J. (1988) *Biochemistry 27*, 820.

Fronticelli, C., Bucci, E., Razynska, A., Sznajder, J., Urbaitis, B., & Gryczynski, Z. (1990) *Eur. J. Biochem.* 193, 331.

Gill, S. J., Richey, B., Bishop, G., & Wyman, J. (1985) *Biophys. Chem. 21*, 1.

Gill, S. J., Di Cera, E., Doyle, M., Bishop, G. A., & Robert, C. H. (1987) *Biochemistry 26*, 3995.

Hayashi, A., Suzuki, T., & Shin, M. (1973) *Biochim. Biophys. Acta 310*, 309.

Imai, K. (1982) *Allosteric Effects in Hemoglobin*, Cambridge University Press, Cambridge, England.

Imaizumi, K., Imai, K., & Tyuma, I. (1978) *J. Biochem. (Tokyo) 83*, 1707.

Johnson, C. R., Gill, S. J., & Peters, K. S. (1992) *Biophys. Chem.* (in press).

Johnson, M. L., Halvorson, H. R., & Ackers, G. K. (1976) *Biochemistry 15*, 5363.

Kilmarten, J. V., Imai, K., Jones, R. T., Faruqui, A. R., Fogg, J., & Baldwin, J. M. (1978) *Biochim. Biophys. Acta 534*, 15.

Koshland, D. E., Jr., Nemethy, G., & Filmer, D. (1966) *Biochemistry 5*, 365.

Magar, M. E. (1972) *Data Analysis in Biochemistry and Biophysics*, Academic Press, New York.

Nasuda-Kouyama, A., Tachibana, H., & Wada, A. (1983) *J. Mol. Biol. 164*, 451.

Ownby, D. W., & Gill, S. J. (1990) *Biophys. Chem. 57*, 238a.

Parody-Morreale, A., Robert, C. H., Bishop, G. A., & Gill, S. J. (1987) *J. Biol. Chem. 262*, 10994.

Perutz, M. F. (1970) *Nature 228*, 726.

Perutz, M. F. (1987) *Acc. Chem. Res. 20*, 309.

Philo, J. S., Adams, M. L., & Schuster, T. M. (1981) *J. Biol. Chem. 256*, 7917.

Rifkind, J. M. (1988) *Advances in Inorganic Biochemistry* (Eichhorn, G. L., & Marzilli, L. G., Eds.) p 155, Elsevier, New York.

Rifkind, J., & Lumry, R. (1967) *Fed. Proc. 26*, 2325.

Robert, C. H., Fall, L., & Gill, S. J. (1988) *Biochemistry 27*, 6835.

Roughton, F. J. W., Otis, A. B., & Lyster, R. L. J. (1955) *Proc. R. Soc. London, Ser. B 144*, 29.

Van Assendelft, O. W., & Zijlstra, W. G. (1975) *Anal. Biochem. 69*, 43.

Vandegriff, K. D., Medina, F., Marini, M. A., & Winslow, R. W. (1989) *J. Biol. Chem. 264*, 17824.

Williams, R. C., & Tsay, K. (1973) *Anal. Biochem. 54*, 137.

Wyman, J. (1948) *Adv. Protein Chem. 4*, 407.

Wyman, J. (1964) *Adv. Protein Chem. 19*, 233.

Wyman, J. (1967) *J. Am. Chem. Soc. 89*, 2202.

Wyman, J. (1984) *Q. Rev. Biophys. 17*, 453.

Wyman, J., & Gill, S. J. (1980) *Proc. Natl. Acad. Sci. U.S.A. 77*, 5239.


**Registry No.** $O_2$, 7782-44-7; $HbA_0$, 54651-57-9.